

Antiferromagnetic Semiconducting Parent Compound of the High Temperature Superconductor $K_xFe_{2-y}Se_2$

Jun Zhao,^{1,2} Huibo Cao,³ E. Bourret-Courchesne,⁴ D. -H. Lee,^{1,4} and R. J. Birgeneau^{1,5}

¹*Department of Physics, University of California, Berkeley, California 94720, USA*

²*Miller Institute for Basic Research in Science, Berkeley, California 94720, USA*

³*Quantum Condensed Matter Division, Oak Ridge National Laboratory, Oak Ridge, TN 37831*

⁴*Materials Sciences Division, Lawrence Berkeley National Laboratory, Berkeley, California 94720, USA*

⁵*Department of Materials Science and Engineering, University of California, Berkeley, California 94720, USA*

Identifying the parent compound and understanding its structural and magnetic properties have been proven to be very important in the study of high temperature (high- T_c) superconductors. For example, the parent compounds of the cuprates are antiferromagnetic (AF) Mott insulators while those of the iron pnictides are AF semi-metals [1, 2]. The recently discovered K-Fe-Se superconductor with coexisting $\sqrt{5} \times \sqrt{5}$ block AF order and superconductivity has caused heated debate in this regard [3–11]. Here we report neutron diffraction experiments which suggest that the parent compound of the K-Fe-Se superconductor is an AF semiconductor with a rhombus type iron vacancy order. Furthermore, the magnetic structure is the same as that in other iron pnictides and the Neel temperature is about 280 K. The superconductivity is induced by electron doping which completely suppresses the AF order. The fact that an antiferromagnetic semiconducting parent material can also lead to high- T_c superconductivity sets a new direction for the search for magnetic high- T_c superconductors.

In the parent compounds of the cuprate high T_c superconductors, it is well established that the magnetic order arises from exchange interactions of local moments driven by strong electron correlations [1]. However, the origin of the magnetism in the iron pnictides is still a matter of debate. It is widely believed that the magnetism is related to Fermi surface scattering, since the AF order is always characterized by a wave vector connecting centers of the electron and hole Fermi surfaces [2]. Alternatively, a local moment picture has also been proposed for the iron pnictides, similar to that of the cuprates [12, 13]. The recently discovered alkali metal intercalated iron selenide superconductors $A_xFe_{2-y}Se_2$ ($A=K, Rb, Cs$) has attracted great interest because they display a variety of properties unprecedented for the cuprates and iron pnictides [3, 11]. For example, ARPES measurements have suggested that their Fermi surface does not have any hole pockets [14–16]. In terms of their magnetic properties, the $A_xFe_{2-y}Se_2$ superconductors are equally unusual. Early work suggested that a strong $\sqrt{5} \times \sqrt{5}$ block AF order coexists with superconductivity [4, 17]; while recently, there has been growing evidence suggesting that the block AF phase is spatially separated from the superconducting phase [7, 18–22] and that superconductivity only exists in a minority phase with no block AF order [8, 23–26]. In addition, ARPES and transport measurements have identified several different phases in the $K_xFe_{2-y}Se_2$ compounds: an insulating phase with a 500 meV band gap (from now on we refer to it as the “insulating” phase), a small gap insulating phase with a 40 meV gap (from now on we refer to it as the “semiconducting” phase), and a superconducting phase with only electron-like Fermi surfaces [7]. In order to clarify whether the mechanism of superconductivity in this system is fundamentally different from that in the iron pnictides or cuprates, a determination of the stoichiometry, lattice structure and magnetic ground states of these different phases and their relationship with superconductivity is crucial.

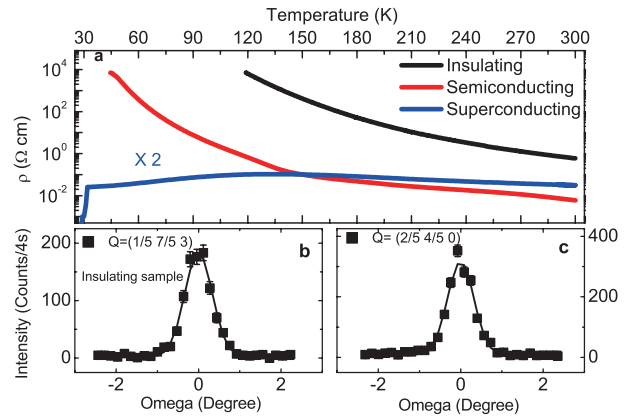


FIG. 1. **Resistivity of various $K_xFe_{2-y}Se_2$ samples, and $\sqrt{5} \times \sqrt{5}$ superstructure reflections of the insulating $K_{0.8}Fe_{1.6}Se_2$.** The Bragg reflections of insulating $K_{0.8}Fe_{1.6}Se_2$ can be fully described with $\sqrt{5} \times \sqrt{5}$ block AF order and iron vacancy order. **a**, In-plane resistivity as a function of temperature for the insulating sample, the semiconducting sample and the superconducting sample with the $T_c=30$ K. The resistivity of the superconducting sample is multiplied by 2. **b**, Magnetic reflection associated with $\sqrt{5} \times \sqrt{5}$ block AF order of the insulating sample. **c**, Nuclear reflection associated with $\sqrt{5} \times \sqrt{5}$ iron vacancy order of the insulating sample. The lattice parameters of the insulating sample are $a=b=5.504(3)$ Å, $c=14.03(6)$ Å at 5 K in the orthorhombic notation. The error bars indicate one standard deviation throughout the paper.

We use neutron diffraction to study the structure, magnetic order and stoichiometry of a series of $K_xFe_{2-y}Se_2$ compounds. High quality single crystals were grown with the Bridgman technique as described elsewhere in detail [27]. The transport properties are characterized by the in-plane resistivity which displays insulating, semiconducting or superconducting behavior (Fig. 1a). These results are similar to those in previous reports [7, 28]. The neutron scattering measurements were carried out on HB-3A four circle single-crystal diffractometer

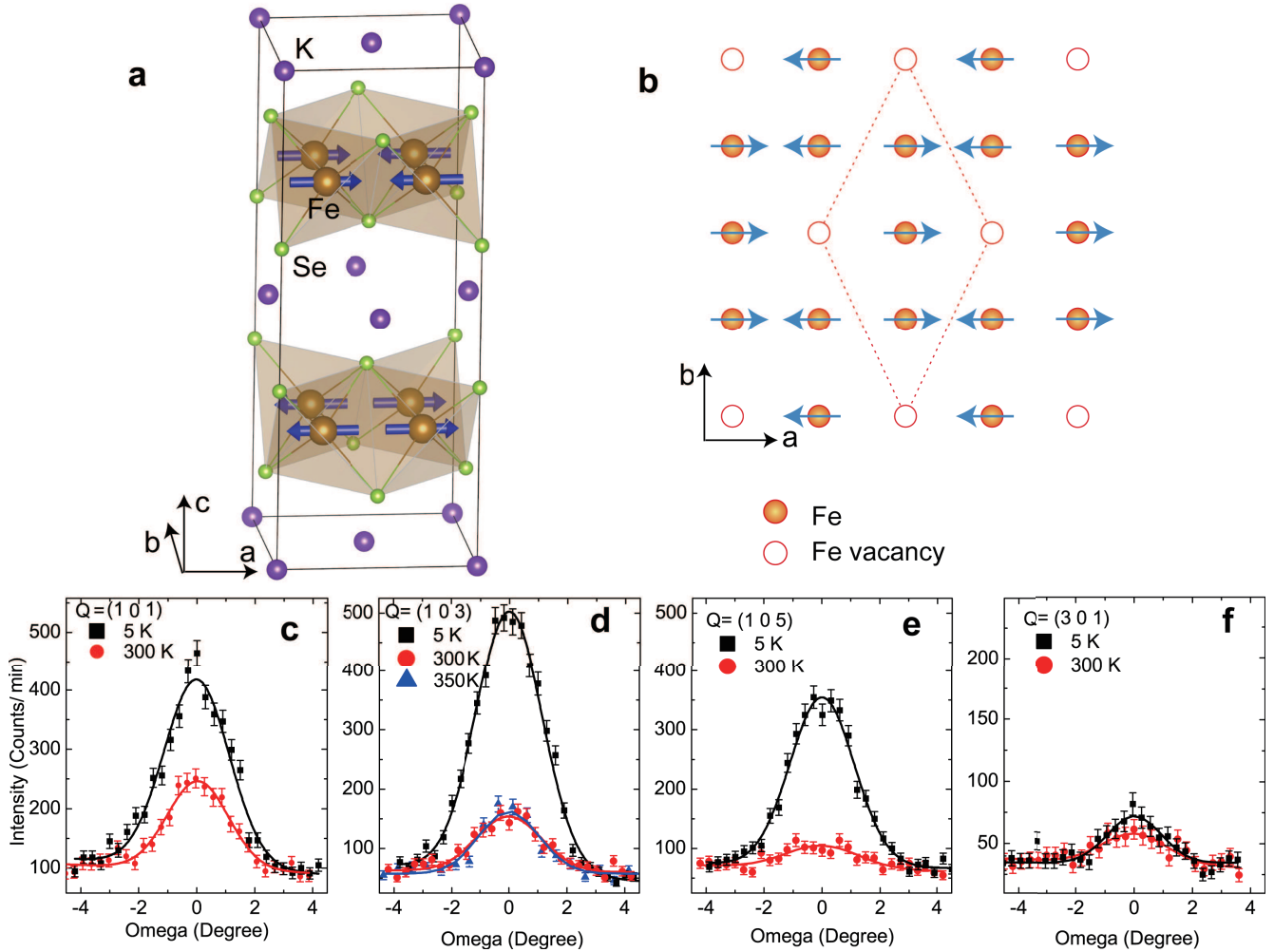


FIG. 2. **Stripe type magnetic order and rhombus iron vacancy order of semiconducting $\text{K}_{0.85}\text{Fe}_{1.54}\text{Se}_2$.** **a**, The three-dimensional stripe type magnetic structure of iron as determined from our neutron diffraction data. **b**, The in-plane magnetic structure and rhombus iron vacancy order. The red dashed line marks the rhombus iron vacancy order. **c-f**, A series of temperature dependence magnetic and nuclear reflections associated with the stripe type magnetic order and rhombus iron vacancy order. The extra intensities appearing at 5 K are associated with development of long range AF order. The residue intensities at 300 K are due to rhombus iron vacancy order. **c**, Omega scans near $Q=(1\ 0\ 1)$; **d**, $Q=(1\ 0\ 3)$; **e**, $Q=(1\ 0\ 5)$; **f**, $Q=(3\ 0\ 1)$.

at the High-Flux Isotope Reactor at the Oak Ridge National Laboratory. The neutron wavelength employed was 1.000 Å using a bent perfect Si-331 monochromator. No higher order neutron reflection is allowed with this experimental setup. We define the wave vector Q at (q_x, q_y, q_z) as $(h, k, l) = (q_x a/2\pi, q_y a/2\pi, q_z c/2\pi)$ reciprocal lattice units (r.l.u.) in the orthorhombic unit cell to facilitate comparison with the iron pnictides. The neutron diffraction data refinements are based on more than 200 magnetic and nuclear reflections with the program FULLPROF [29].

Fig. 1b and 1c display the magnetic and nuclear peaks associated the $\sqrt{5} \times \sqrt{5}$ reconstruction at 5 K in the insulating sample. These superstructure peaks can be fully described with the $\sqrt{5} \times \sqrt{5}$ block AF order and iron vacancy order, consistent with the results reported previously [4–6]. Our Rietveld refinements suggest that this sample has a pure $\text{K}_2\text{Fe}_4\text{Se}_5$ (245)

phase (or $\text{K}_{0.8}\text{Fe}_{1.6}\text{Se}_2$) with a magnetic moment $\sim 3.2(1) \mu_B$ (Table 1).

The most striking discovery is that in addition to the $\sqrt{5} \times \sqrt{5}$ superstructure peaks, we also observed in the semiconducting sample magnetic Bragg peaks at the $\sqrt{2} \times \sqrt{2}$ positions at 5K (Fig. 2c-2f). Here $\sqrt{2} \times \sqrt{2}$ corresponds to $(10l)$ in the orthorhombic unit cell shown in Fig. 2a. These peak intensities are significantly suppressed on warming to 300 K, indicative of a magnetic phase transition (Fig. 2c-2f). The detailed temperature dependences of the (103) and (105) peaks show clear kinks at around $T_N = 280$ K, suggesting a second order phase transition (Fig. 3a and 3b). Interestingly, some weak superstructure peaks are still present above 280 K; these peaks exhibit negligible temperature dependence between 280 K and 450 K (Fig. 2 and 3), demonstrating that the residual scattering is nuclear in origin. Our Rietveld refinements reveal

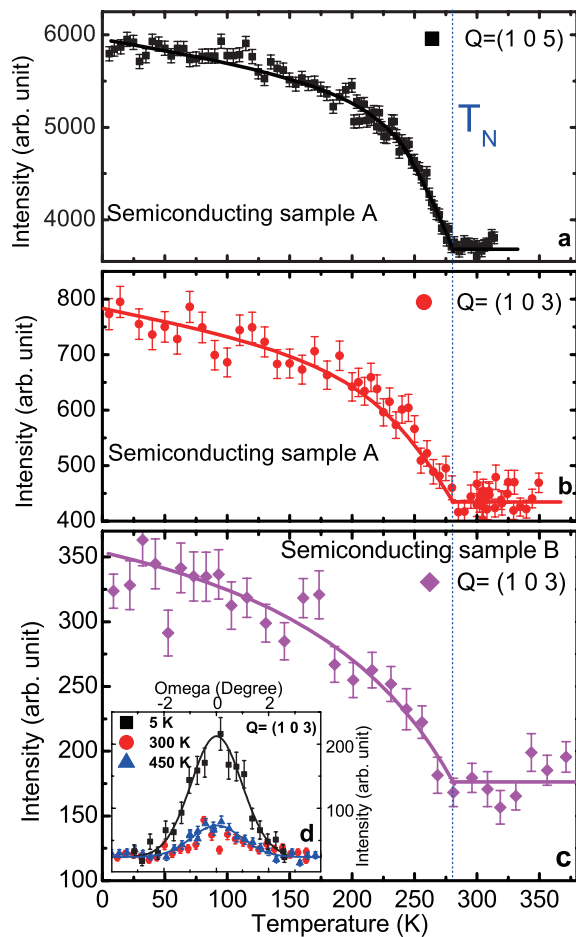


FIG. 3. **Magnetic order parameter in two different semiconducting $K_{0.85}Fe_{1.54}Se_2$ samples.** The temperature dependence of the magnetic Bragg peak intensities display second order magnetic phase transition with the Neel temperature $T_N = 280$ K. **a**, Temperature dependence of $Q=(1\ 0\ 5)$ magnetic peak of the sample A. **b**, Temperature dependence of $Q=(1\ 0\ 3)$ magnetic peak of the sample A. **c**, Temperature dependence of $Q=(1\ 0\ 3)$ magnetic peak of the sample B. **d**, Temperature dependence of the omega scans of $Q=(1\ 0\ 3)$ peak of sample B. The peak exhibits little temperature dependence between 300 K and 450 K, indicating the residue intensity above 280 K is associated with the rhombus iron vacancy order.

that the scattering above 280 K is associated with a rhombus iron vacancy order in the $ThCr_2Si_2$ -type (122) phase as shown in Fig. 2a and 2b.

In order to determine the detailed magnetic structure in the 122 phase, we analyzed the integrated intensity of a series of magnetic Bragg reflections. The peak intensity increases from (1 0 1) to (1 0 3), and then decreases at (1 0 5), implying that the magnetic moments lie in the ab plane, which is completely different from the $\sqrt{5} \times \sqrt{5}$ block AF order with the moment along c axis. Rietveld refinements reveal that the magnetic peak intensities follow the Fe^{2+} magnetic form factor and can be described with the same stripe type magnetic structure of the iron pnictide parent compounds (Fig. 2a and 2b). The Fe moment is antiferromagnetically ordered along the a and c

axis and ferromagnetically ordered along the b axis with the moment parallel to the a axis. Here the a axis is parallel to the short diagonal of the iron vacancy rhombus (Fig. 2a and 2b).

By taking into account the $\sqrt{5} \times \sqrt{5}$ iron vacancy ordered phase (245 phase) together with the 122 phase with the stripe AF order and the rhombus iron vacancy order discussed above, we can completely determine the magnetic and lattice structure parameters in the semiconducting sample (Table 1). Based on our refinements, the fractions of the 245 phase and 122 phase in the semiconducting sample amount to $\sim 74.8\%$ and $\sim 25.2\%$, respectively. The refined stoichiometry of the 122 phase is $K_{0.85}Fe_{1.54}Se_2$. The iron moments of the stripe type AF order and block AF order are $2.8(1)\mu_B$ and $3.4(1)\mu_B$, respectively. We notice that the moment and stoichiometry of block AF order phase in the semiconducting sample are very close to those of pure 245 phase of the insulating sample, which is consistent with the fact that they have similar Neel temperatures (Table 1) [7, 28]. In a similar $K_xFe_{2-y}Se_2$ sample, ARPES measurements also observed two different phases: an insulating phase with a 500 meV gap and a semiconducting phase with a 40 meV gap [7]. Based on the above observations, we identify the stripe AF ordered 122 phase as the semiconducting phase discussed earlier. Remarkably, a first principle calculation has predicted the same magnetic structure and iron vacancy order in a 122 type structure in $KFe_{1.5}Se_2$ [30]. The same calculation also suggests that this system is a band semiconductor with a 121 meV gap [30]. Therefore, we believe that the $K_{0.85}Fe_{1.54}Se_2$ phase with 122 structure discovered here is an antiferromagnetic band semiconductor, in contrast to the Mott insulating cuprates and metallic iron pnictides. We note that the refined potassium concentration deviates slightly from the commensurate $KFe_{1.5}Se_2$ phase, which could be due to the presence of disordered and localized vacancies or interstitials.

In addition to the results shown in Fig. 2, Fig. 3a and 3b, we also performed similar measurements in another semiconducting sample (semiconducting sample B). Very similar stripe type AF structure and magnetic order parameter temperature dependence are also observed (Fig. 3c), demonstrating that the stripe type AF order is an intrinsic property of semiconducting samples.

We now discuss our results in the superconducting sample. Several STM measurements have suggested that superconducting samples contain both an insulating $\sqrt{5} \times \sqrt{5}$ iron vacancy order phase and a superconducting 122 type phase with $\sqrt{2} \times \sqrt{2}$ superstructure which are spatially separated [8, 23, 24]. Our refinements on the diffraction data suggest that the fractions of 245 phase and 122 phase (refined stoichiometry $K_{0.88}Fe_{1.63}Se_2$) amount to $\sim 83.3\%$ and $\sim 16.7\%$, respectively (Table 1). Interestingly, while the block AF order (refined moment $3.3(1)\mu_B$) in this sample is still very close to that of pure 245 phase, the stripe type AF order and rhombus iron vacancy order are completely suppressed in the superconducting sample. Although some very weak $\sqrt{2} \times \sqrt{2}$ reconstruction reflections are still present (Fig. 4b-4f), their integrated intensities cannot be described with stripe AF order or

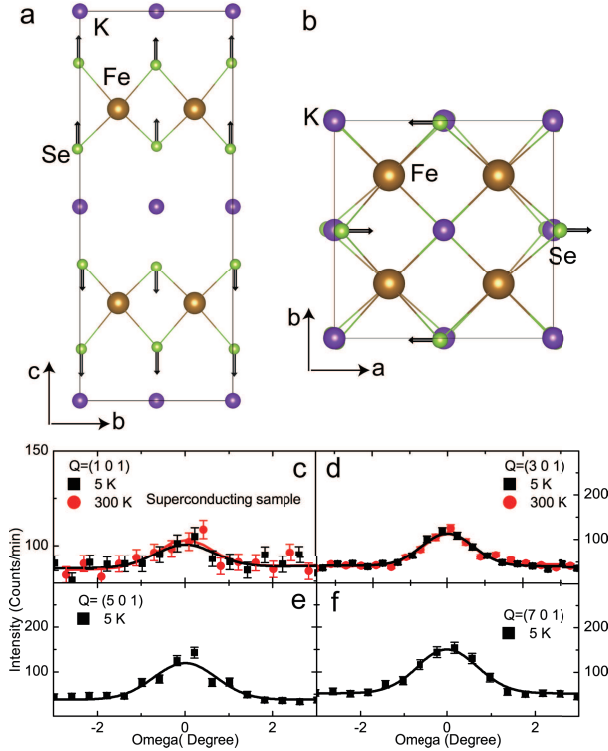


FIG. 4. $\sqrt{2} \times \sqrt{2}$ Se distortion in the 122 structure of the superconducting phase $\text{K}_{0.88}\text{Fe}_{1.63}\text{Se}_2$ ($T_c = 30$ K). **a**, **b**, Schematic diagram of Se distortion; the arrows indicate the directions of the atom displacements with respect to perfect lattice. **a**, Se distortion along c axis. **b** Se distortion along a axis. **c-f**, $\sqrt{2} \times \sqrt{2}$ reflections associated with Se distortion. The Bragg peak intensity increases as increasing h , suggesting it is nuclear in origin. **c**, Omega scans of $Q = (1\ 0\ 1)$ Bragg peak displays little temperature dependence between 5 K to 300 K, indicating the stripe type AF order is completely suppressed. The weak scattering left is associated with Se distortion. **d**, Temperature dependence of $Q = (3\ 0\ 1)$ Bragg peak. **e**, $Q = (5\ 0\ 1)$ Bragg peak at 5 K. **f**, $Q = (7\ 0\ 1)$ Bragg peak at 5 K.

rhombus iron vacancy order. These weak reflections display negligible temperature dependence between 5 K and 300 K, indicating that they are nuclear in origin. Our Rietveld refinement suggests that this $\sqrt{2} \times \sqrt{2}$ superstructure could be due to the Se distortion as illustrated in Fig. 4a and 4b. We note that the iron and potassium concentrations in the superconducting sample are higher than those of 122 phase of the semiconducting sample, which naturally implies that the extra iron and potassium would introduce electron doping and thus suppress the stripe type AF order. The extra iron is also expected to suppress the rhombus iron vacancy order. Therefore, our findings strongly indicate that the magnetic and iron vacancy ordered semiconducting $\text{K}_{0.85}\text{Fe}_{1.54}\text{Se}_2$ is the real parent compound of this superconductor. On the other hand, the magnetic moment of the $\sqrt{5} \times \sqrt{5}$ block AF order in 245 phase is essentially unchanged in the insulating, semiconducting and superconducting samples, implying that this phase is not directly relevant to the superconductivity (Table 1).

TABLE I. Refined structure parameters of 245 phase and 122 phase in insulating, semiconducting and superconducting $\text{K}_x\text{Fe}_{2-y}\text{Se}_2$

	Superconductor	Semiconductor	Insulator
Phase	122 , 245	122 , 245	245
Phase ratio	16.7% : 83.3%	25.2% : 74.8%	1
Moment (μ_B)	0 , 3.3(1)	2.8(1) , 3.4(1)	3.2(1)
K Occupancy	0.88(6) , 0.84(7)	0.85(7) , 0.80(6)	0.80(7)
Fe Occupancy	1.63(3) , 1.60(1)	1.54(2) , 1.60(1)	1.60(1)
Se Occupancy	2 , 2	2 , 2	2
R_1	0.0334, 0.0363	0.0475, 0.0555	0.0384
wRF^2	0.0828, 0.0763	0.0641, 0.116	0.0719
χ^2	0.894, 0.533	0.539, 1.017	0.392

In summary, our neutron diffraction data strongly suggest that the parent compound of the K-Fe-Se superconductor is a semiconductor with a simple stripe type antiferromagnetic order and a rhombus iron vacancy order in the background of the 122 type structure (Fig. 2a and 2b). The magnetic structure, iron vacancy structure and magnetic moment ($\sim 2.8 \mu_B$) of $\text{K}_{0.85}\text{Fe}_{1.54}\text{Se}_2$ are consistent with first principle calculations that suggest a band semiconducting ground state in this system [30]. We also show that the superconductivity is induced with increasing iron and potassium concentrations which suppress the AF order and iron vacancy order, resulting in a phase diagram quite similar to those of other high T_c superconductors. These results are in agreement with the ARPES measurements which suggested that the superconductivity can be obtained by electron doping the semiconducting phase [7].

The discovery of a band semiconducting AF parent compound of high T_c superconductor has profound implications. Clearly, a naive Fermi surface nesting picture is not applicable for this system. Ref.[30] suggests the semiconducting antiferromagnet can be viewed at the atomic level as due to the exchange interactions bridged by Se between Fe local moments. We also notice that the magnetic moment ($2.8 \mu_B$) and Neel temperature (280 K) of semiconducting $\text{K}_{0.85}\text{Fe}_{1.54}\text{Se}_2$ are much higher than those of 122 iron pnictides [2]. This suggests that correlation physics plays a larger part in the magnetism for this system. The large magnetic moment in $\text{A}_x\text{Fe}_{2-y}\text{Se}_2$ may also explain why the magnetic resonance intensity in phase-separated $\text{Rb}_x\text{Fe}_{2-y}\text{Se}_2$ is comparable to that of the phase pure superconductor $\text{BaFe}_{2-x}\text{Ni}_x\text{As}_2$ [31, 32]. In any case, the semiconducting antiferromagnet we discovered in this work interpolates between the antiferromagnetic Mott insulator of the cuprates and the antiferromagnetic semimetal of the iron pnictides. It might open a new window for finding new high T_c superconductors.

We thank J.P. Hu for helpful discussions. This work is supported by the Director, Office of Science, Office of Basic Energy Sciences, U.S. Department of Energy, under Contract No. DE-AC02-05CH11231 and Office of Basic Energy Sciences US DOE DE-AC03-76SF008. Jun Zhao is supported by a fellowship from Miller Institute for Basic Research in Science. D.-H. Lee is supported by DOE Grant No. DE-AC02-

-
- [1] Lee, P. A., Nagaosa, N. & Wen, X.-G. Doping a Mott insulator: Physics of high-temperature superconductivity. *Rev. Mod. Phys.* **78**, 17-85 (2006).
- [2] D. Johnston The puzzle of high temperature superconductivity in layered iron pnictides and chalcogenides. *Advances in Physics* **59** 803 (2010).
- [3] Guo, J. *et al.* Superconductivity in the iron selenide $K_xFe_2Se_2$ ($0 \leq x \leq 1.0$). *Phys. Rev. B* **82**, 180520 (2010).
- [4] Bao, W. *et al.* A novel large moment antiferromagnetic order in $K_{0.8}Fe_{1.6}Se_2$ superconductor. *Chinese Phys. Lett.* **28** 086104 (2011).
- [5] Ye, F. *et al.* Common crystalline and magnetic structure of superconducting $A_2Fe_4Se_5$ ($A=K,Rb,Cs,Tl$) single crystals measured using neutron diffraction. *Phys. Rev. Lett.* **107**, 137003 (2011)
- [6] Wang, M. *et al.* Antiferromagnetic order and superlattice structure in nonsuperconducting and superconducting $Rb_yFe_{1.6+x}Se_2$. *Phys. Rev. B* **84**,094504 (2011).
- [7] Yan, Y. J. *et al.* Electronic identification of the parental phases and mesoscopic phase separation of $K_xFe_{2-y}Se_2$ superconductors. *Phys. Rev. X* **1**,021020 (2011).
- [8] Li, W. *et al.* KFe_2Se_2 is the parent compound of K-doped iron selenide superconductors. Preprint at <http://arxiv.org/abs/1204.1588>
- [9] Fang, M. H. *et al.* Fe-based high temperature superconductivity with $T_c=31$ K bordering an insulating antiferromagnet in $(Tl,K)Fe_xSe_2$ Crystals. *Eur. Phys. Let.* **94**, 27009 (2011).
- [10] Sales, C. B. *et al.* Unusual phase transitions and magnetoelastic coupling in $TlFe_{1.6}Se_2$ single crystals *Phys. Rev. B* **83**, 224510 (2011)
- [11] Mazin, I. Iron superconductivity weathers another storm. *Physics* **4**, 26 (2011)
- [12] Fang, C. *et al.* Theory of electron nematic order in $LaFeAsO$. *Phys. Rev. B* **77**, 224509 (2008).
- [13] Si, Q. *et al.* Strong correlations and magnetic frustration in the high T_c iron pnictides. *Phys. Rev. Lett.* **101**, 076401 (2008).
- [14] Zhang, Y. *et al.* Nodeless superconducting gap in $A_xFe_2Se_2$ ($A=K,Cs$) revealed by angle-resolved photoemission spectroscopy *Nature Materials* **10** 273-277 (2011)
- [15] Mou, D. X. *et al.* Distinct Fermi surface topology and nodeless superconducting gap in a $Tl_{0.58}Rb_{0.42}Fe_{1.72}Se_2$ Superconductor *Phys. Rev. Lett.* **106** 107001 (2011)
- [16] Qian, T. *et al.* Absence of a holelike Fermi surface for the iron-based $K_{0.8}Fe_{1.7}Se_2$ superconductor revealed by Angle-Resolved Photoemission Spectroscopy *Phys. Rev. Lett.* **106** 187001 (2011)
- [17] Shermadini,Z. *et al.*, Coexistence of magnetism and superconductivity in the iron-based compound $Cs_{0.8}(FeSe_{0.98})_2$. *Phys. Rev. Lett.* **106**, 117602 (2011).
- [18] Shermadini,Z. *et al.* Superconducting properties of single-crystalline $A_xFe_{2-y}Se_2$ ($A=Rb, K$) studied using muon spin spectroscopy. *Phys. Rev. B.* **85**, 100501(R) (2012)
- [19] Ksenofontov, V. *et al.* Phase separation in superconducting and antiferromagnetic $Rb_{0.8}Fe_{1.6}Se_2$ probed by Mossbauer spectroscopy. *Phys. Rev. B.* **84**, 180508(R) (2011)
- [20] Yuan, R. H. *et al.* Nanoscale phase separation of antiferromagnetic order and superconductivity in $K_{0.75}Fe_{1.75}Se_2$. *Scientific Reports* **2**, 221 (2011)
- [21] Ricci, A. *et al.* Nanoscale phase separation in the iron chalcogenide superconductor $K_{0.8}Fe_{1.6}Se_2$ as seen via scanning nanofocused x-ray diffraction. *Phys. Rev. B.* **84**, 060511(R) (2011)
- [22] Charnukha, A. *et al.* Optical conductivity of superconducting $Rb_2Fe_4Se_5$ single crystals. *Phys. Rev. B.* **85**, 100504 (2012)
- [23] Cai, P. *et al.* Imaging the coexistence of superconductivity and a charge density modulation in $K_{0.73}Fe_{1.67}Se_2$ superconductor. *Phys. Rev. B.* **85**, 094512 (2012)
- [24] Li, W. *et al.* Phase separation and magnetic order in K-doped iron selenide superconductor. *Nat. Phys.* **8**,126-130(2012)
- [25] Texier, Y. *et al.* NMR in the 245 iron-selenides $Rb_{0.74}Fe_{1.6}Se_2$: Phase separation between an antiferromagnet and a superconducting $Rb_{0.3}Fe_2Se_2$. Preprint at <http://arXiv.org/abs/1203.1834>.
- [26] Borisenko, S. V. *et al.* Cigar Fermi surface as a possible requisite for superconductivity in iron-based superconductors. Preprint at <http://arxiv.org/abs/1204.1316>.
- [27] Zhao, J. *et al.*, unpublished
- [28] Yan, Y. J. *et al.* Electronic and magnetic phase diagram in $K_xFe_{2-y}Se_2$ superconductors. Preprint at <http://arxiv.org/abs/1104.4941> (2011).
- [29] Rodriguez-Carvajal, J. Recent advances in magnetic structure determination by neutron powder diffraction. *Physica B* **192**, 55 (1993)
- [30] Yan, X.-W., Gao, M., Lu, Z.-Y. & Xiang, T. Electronic structures and magnetic order of ordered-Fe-vacancy ternary iron selenides $TlFe_{1.5}Se_2$ and $AFe_{1.5}Se_2$ ($A=K, Rb, \text{ or } Cs$). *Phys. Rev. Lett.* **106**, 087005 (2011).
- [31] Park, J. T. *et al.* Magnetic resonant mode in the low-energy spin-excitation spectrum of superconducting $Rb_2Fe_4Se_5$ single crystals. *Phys. Rev. Lett.* **107**,177005 (2011).
- [32] Chi, S. X. *et al.* Inelastic neutron-scattering measurements of a three-dimensional spin resonance in the FeAs-Based $BaFe_{1.9}Ni_{0.1}As_2$ superconductor. *Phys. Rev. Lett.* **102**,107006 (2009).